COMMUNICATION

Facile Synthesis of Nitrogen-Doped Graphene via Pyrolysis of Graphene Oxide and Urea, and its Electrocatalytic Activity toward the Oxygen-Reduction Reaction

Ziyin Lin, Gordon Waller, Yan Liu, Meilin Liu, and Ching-Ping Wong**

As a single layer of carbon atoms covalently bonded into a hexagonal lattice, graphene exhibits a wide range of fascinating physical properties, such as a remarkable charge-carrier mobility,[1] excellent thermal conductivity,[2] and a high optical transparency.[3] These properties lead to very promising applications of graphene in electronic devices,[4] transparent electrodes,[5] and energy-storage devices.[6,7] Recently, it was found that graphene has an extraordinary catalytic activity.[8–14] For example, N-doped graphene has a high catalytic activity toward the oxygen-reduction reaction (ORR).[8] Furthermore, graphene oxide (GO), an important derivative of graphene, is an efficient catalyst for oxidation and hydration reactions of various alcohols,[9] whereas reduced GO can be used for catalyzing the hydrogenation of nitrobenzene.[10] Studies have shown that the heteroatoms in graphene derivatives, such as N and O, play a critical role in their catalytic activities.[10,15,16] Thus, the introduction of dopants into the graphene lattice has been the focus of much research in order to achieve a high catalytic activity toward target reactions.

Among various doped graphenes, nitrogen-doped graphene (NG) has attracted much attention because of its high catalytic activity toward the ORR – the electrode reaction that often limits the performance of the cathode in a fuel cell or a metal-air battery. Conventional Pt-based catalysts have a high intrinsic catalytic activity toward the ORR, but suffer from the drawbacks of high cost, poor long-term stability, and susceptibility to the crossover effect, which hinder the commercial viability of Pt-loaded fuel cells.[17] Thus the search for an alternative catalyst, such as NG, is of great importance in replacing these expensive Pt-based catalysts.

To prepare NG, chemical-vapor deposition in the presence of N-containing precursors is the most-common method;[18] arc discharge of graphite electrodes in a H_2/pyridine or H_2/NH_3 atmosphere can also produce NG.[19] However, the extremely low yield and high cost of these methods limit their application only to fundamental studies. Later, it was found that GO can be used as a platform for N incorporation via thermal annealing with NH_3[20,21] or nitrogen plasma treatment.[22,23] However, these methods involve either toxic precursors or sophisticated equipment. Therefore, developing a low-cost, scalable, and eco-friendly method is still of great interest.

In this report, NG is successfully prepared from GO and a solid N precursor, urea, both of which are low-cost and being manufactured in large quantities.[24] With its high N content (46 wt%), urea can react with oxygen-containing functional groups and has been used for the nitridation of various materials such as activated carbon and metal oxide particles.[25–27] Well-mixed GO and urea were pyrolyzed at 800 °C in an inert environment as described in the supporting information. During the pyrolysis, the GO was thermally reduced and N atoms were doped into the graphitic lattice, producing N-doped reduced GO, which is called NG in this work.

The morphology of the resulting NG was characterized by scanning electron microscopy (SEM) and transmission electron microscopy (TEM). Both the typical graphene structure (Figure S1a, Supporting Information) and a highly defective structure (Figure S1b) were observed under SEM. As shown in a typical TEM image (**Figure 1**a), the highly wrinkled NG had a low contrast under the electron beam, indicating a small thickness.

Raman microscopy offered clear evidence of N-doping in the graphene lattice. As shown in Figure 1b, the G peaks of the GO, graphene, and NG appeared at 1600, 1588, and 1580 cm^{-1}, respectively. The downshift of the G peak from GO to graphene can be attributed to the restoration of the conjugated structure during pyrolysis.[28] The further downshift of the G peak in NG concurs with previous reports of NG from other methods, and may be related to the electron-donating capability of N heteroatoms (a detailed discussion is given in the supporting information).[20,29,30] In addition, the I_D/I_G ratio in the Raman spectra was used to evaluate the disorder in the graphene materials. It was found that the I_D/I_G ratio in GO was 1.10, which increased slightly to 1.13 for graphene and to 1.15 for NG. The increased I_D/I_G ratio probably resulted from the generation of smaller nanocrystalline graphene domains,[31] the loss of carbon atoms by the decomposition of oxygen-containing groups,[32] and the incorporation of N heteroatoms.[29]

The chemical structure of NG was investigated further using Fourier transform IR (FTIR) spectroscopy. As shown in Figure 1c, the GO showed distinct peaks at ≈3420 (broad), ≈1725, and ≈1625 cm^{-1}, which could be attributed to hydroxyls, carbonyls, and absorbed water, respectively.[6] Urea has characteristic peaks at 3320 and 3420 cm^{-1} (amino groups), and 1680 cm^{-1} (carbonyls). In the FTIR spectra of NG, no peaks relating to

Z. Lin, G. Waller, Y. Liu, Prof. M. Liu, Prof. C.-P. Wong
School of Materials Science and Engineering
Georgia Institube of Technology
771 Ferst Drive, Atlanta, Georgia, 30332, USA
E-mail: meilin.liu@mse.gatech.edu;
cp.wong@mse.gatech.edu
Prof. C.-P. Wong
Department of Electronic Engineering
The Chinese University of Hong Kong, Hong Kong

DOI: 10.1002/aenm.201200038

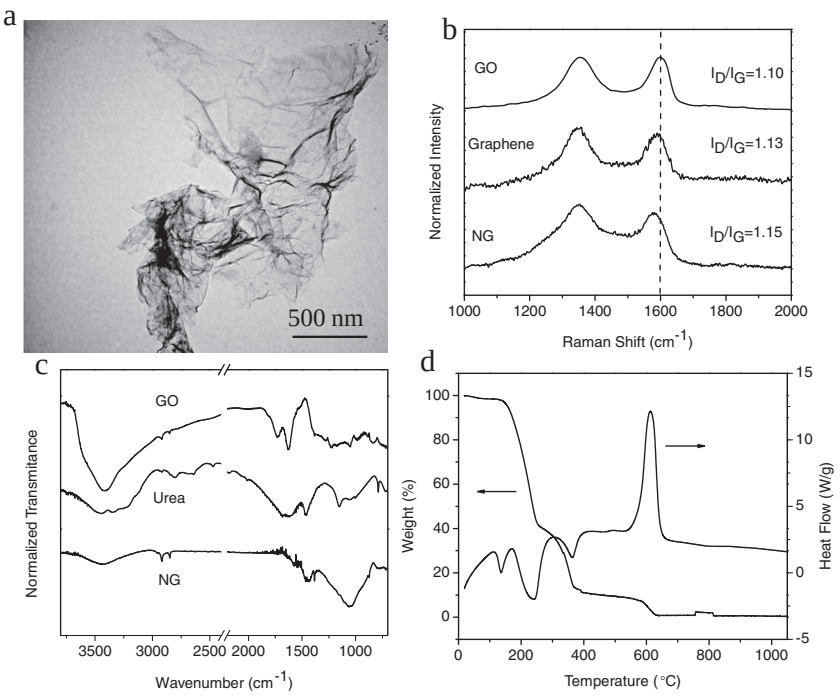

Figure 1. a) TEM of nitrogen-doped graphene (NG). b) Raman spectra of GO, graphene, and NG. c) FTIR spectra of GO, urea, and NG. d) SDT curve of GO-urea mixture.

X-ray photoelectron spectroscopy (XPS) was used to characterize the elemental composition of the NG. As shown in **Figure 2**, the N content was found to be 7.86 at% from the survey spectrum, which is close to the 8.35 at% determined by chemical analysis. The high-resolution C1s peak was centered at 284.8 eV, with a tail at higher binding energies, indicating the existence of carbon atoms connected to N and O heteroatoms. Peak deconvolution showed that there was 74.3% C=C, 17.5% C=N & C–O, 5.9% C–N & C=O, and 2.3% O–C=O. The high-resolution N 1s could be deconvoluted into four components: 44.4% pyridinic N (N-6, N in 6-member ring), 21.2% pyrrolic N (N-5, N in 5-member ring), 24.0% graphitic N (N-G, N in graphene basal plane), and 10.5% oxidized N (N-O). A schematic structure of the NG showing the bonding configurations of the N atoms is given in Figure S3a. Moreover, the high-resolution O 1s spectrum could be fitted with two peaks at ≈532.2 and ≈536.0 eV corresponding to hydroxyls and absorbed water, respectively.

The XPS was particularly useful to study the evolution of N functionalities during the pyrolysis and gain insight into the pathway of N doping. The N precursor, urea, has a simple structure and only one type of N in amino groups (N–H); however the structure of the resulting NG is rather complex, with various amino groups and carbonyls could be observed, indicating that these groups decomposed during pyrolysis. Moreover, a broad peak at ≈1100 cm^{-1} appeared, probably due to the formation of N–C bonds and the residual C–O groups.

Figure 1d shows the simultaneous-differential-scanning-calorimetry (DSC)/thermogravimetric-analysis (SDT) curve, which was used to monitor the physical changes and chemical reactions during the pyrolysis of the GO/urea mixture. The evaporation of water molecules absorbed on the GO resulted in a slight weight loss below 100 °C, and the melting of the urea led to an endothermic peak at ≈136 °C. Two dramatic weight losses were observed between ≈150 –250 °C and ≈300 –370 °C, and were accompanied by large endothermic peaks centered at ≈240 °C and ≈360 °C, respectively. The chemical reaction of the urea decomposition at these temperatures was found to be very complicated, with various reaction intermediates and products such as cyanuric acid, ammelide, and melamine.[33] Moreover, the decomposition of the labile oxygen-containing groups occurred at ≈200 °C. At temperatures between 370 and 560 °C, a gradual weight loss was noted, due to the slow decomposition of the GO and urea derivatives. The complete decomposition of the GO/urea mixture occurred at ≈580–630 °C, with an exothermic peak at ≈610 °C.

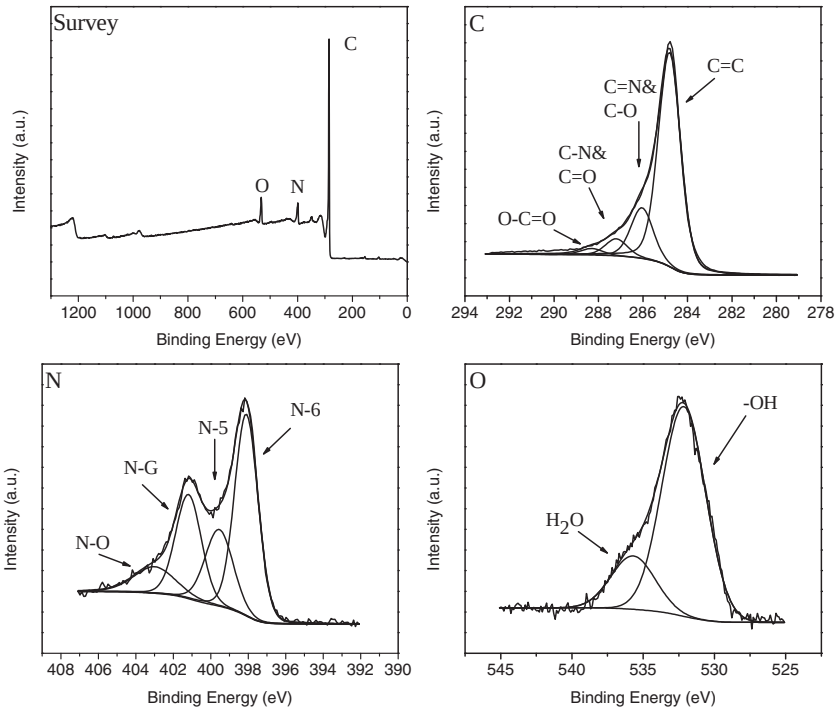

Figure 2. XPS spectra of NG: survey spectrum and high-resolution C 1s, N 1s and O 1s spectra.

N functionalities. Among these functionalities, N-G represents the N atoms doped into the graphitic basal plane, and has been found to be responsible for the ORR catalytic activity of N-doped carbon materials.[15,34] Other N functionalities mainly existed on the edges of the NG, and may play minor roles in the ORR. It was found that the N-G peak at 401.2 eV became increasingly obvious at higher pyrolysis temperatures (Figure S2) as a result of the reconstruction of the NG structure and transformations of the N functionalities. The favorable formation of N-G at high temperatures can be attributed to its thermal stability, higher than that of N-6 and N-5.[35] Moreover, the change of shape of the N 1s spectrum was accompanied by a gradual decrease of the N content (Figure S2, inset). The N content was 13.81% at 400 °C and slowly decreased to 10.88% at 600 °C, 7.86% at 800 °C, and 6.70% at 900 °C.

There are two possible pathways for N-doping during pyrolysis. The first pathway is via chemical reactions of the urea with surface functional groups and subsequent thermal transformations during the pyrolysis. For example, the oxygen-containing functional groups on the GO (hydroxyls, carboxyls) can interact with the amino groups in the urea, contributing to the incorporation of N into the graphene lattice. These N atoms probably exist on the edges, in the form of N-6 and N-5, at the initial stage of pyrolysis, and then transform to N-G at higher temperatures.[36] This process is schematically shown in Figure S3b. Another possible pathway for N-doping is that carbon nitride, produced by the decomposition of the N precursors, acts as an intermediate for the formation of a N dopant in the NG.[37] Although the preparation of carbon nitride from urea has been reported,[38] this pathway has a minor contribution here because: 1) the yield of carbon nitride from urea is very low;[33] 2) the decomposition of carbon nitride (incorporation of N into graphene) occurs below 700 °C, typically leading to a sharp drop of the N content at these temperatures[37] (this is contradictory to the gradually decreased N content observed in the XPS characterizations); and 3) FTIR spectroscopy has confirmed the absence of the signature peak for carbon nitride at ≈810 cm^{-1} (triazine ring),[39] indicating that it is unlikely that carbon nitride is involved in this process.

Figure 3 shows electrochemical characterizations of NG as a metal-free catalyst for the ORR. In a nitrogen-saturated KOH solution, a clean capacitive CV background was seen (Figure 3a). The introduction of oxygen led to a large cathodic current with a peak at ≈–0.32 V, indicating the catalytic activity of the NG. The onset potential for the ORR is an important criterion to evaluate the activity of an electrocatalyst. As shown in Figure 3b, the graphene control sample showed a positively shifted onset potential at –0.18 V, compared with –0.24 V measured on glassy carbon (GC) and ≈–0.4 V measured on CVD-grown graphene,[8] probably due to the existence of a large amount of holes and edges, which have a higher electrochemical activity than the basal plane. However, the NG showed a much-higher activity, as evidenced by the onset potential of –0.10 V, which can be attributed to the effect of N-doping. The ORR on a catalyst surface can either produce peroxide as the product, through a two-electron process, or water, through a four-electron process. It is obvious that the four-electron pathway is more efficient and favorable. The number of the electron transfer per oxygen molecule on NG was determined from rotating-disk-electrode (RDE) measurements, as shown in Figure 3c. The Koutecky–Levich equation was used to analyze the number of the electron transfer:[8]

$$\frac{1}{J} = \frac{1}{J_L} + \frac{1}{J_K} = \frac{1}{B\omega^{1/2}} + \frac{1}{J_K}$$

$$B = 0.2nFC_0 (D_0)^{2/3} \nu^{-1/6}$$

In the Koutecky–Levich equation, J, J_L, J_k are the measured current density, the diffusion-limiting current density, and the kinetic-limiting current density, respectively; ω is the rotation speed in rpm, F is the Faraday constant (96 485 C mol^{-1}), D_0 is the diffusion coefficient of oxygen in 0.1 M KOH (1.9×10^{-5} cm^2 s^{-1}), υ is the kinetic viscosity (0.01 cm^2 s^{-1}), and C_0 is the bulk concentration of oxygen (1.2×10^{-6} mol cm^{-3}). 0.2 is a constant when the rotation speed is expressed in rpm. From the fitting results shown in Figure 3d, it was found that the ORR on NG is dominated by an efficient four-electron process with water as the product. The number of the electron transfer was 4.0 at –0.5 V, which gradually decreased to 3.6 at –1.0 V. In addition, the reliability tests revealed that the NG had a high cycling stability and tolerance to the crossover effect. As shown in Figure 3e, after 2000 consecutive CV cycles in oxygen-saturated KOH, the CV did not show a significant change in shape and area, which is in contrast to the loss of the active surface area for a Pt/C catalyst (Figure S4a). The high stability of the NG can be attributed to the strong covalent bonds between the active sites and the graphitic lattice. Moreover, methanol, a common fuel for fuel cells, was added to the KOH electrolyte to examine the resistance of NG to the crossover effect. As shown in Figure 3f, the CV of NG in the presence of 3 M methanol did not change much, indicating that methanol did not interfere with the ORR reaction on the cathode. However, oxidation of the methanol occurred on the Pt/C surface, which greatly compromised the fuel-cell efficiency (Figure S4b). From these electrochemical characterizations, it can be seen that the catalytic performance of our NG is comparable to those reported previously (Table S1), and was not compromised by the scale-up.

In conclusion, we have developed a simple method for effective doping of N atoms into the graphene lattice by pyrolyzing GO with urea. The morphology, structure, and composition of NG were characterized using SEM, TEM, Raman spectroscopy, and XPS, etc. The total N content in the NG was up to 7.86%, with a high percentage of N-G. Electrochemical tests showed that the NG has high catalytic activity toward the ORR and favors a four-electron pathway. Good stability and the anticrossover property were also observed, superior to Pt/C catalysts.

Experimental Section

Materials Synthesis: The GO was prepared using the Hummers' method. The GO (50 mg) was dispersed in water (100 mL) by ultrasonication. Then, urea (0.25 g) was added into the GO solution, and the mixture was stirred at 500 rpm until complete dissolution of the urea. The solution was dried at 55 °C. The dried GO/urea mixture was pyrolyzed at 800 °C for 30 min in an Ar atmosphere to produce NG. Pure GO was also pyrolyzed under the same conditions. The thermally reduced GO is called graphene in this work and was used as a control sample.

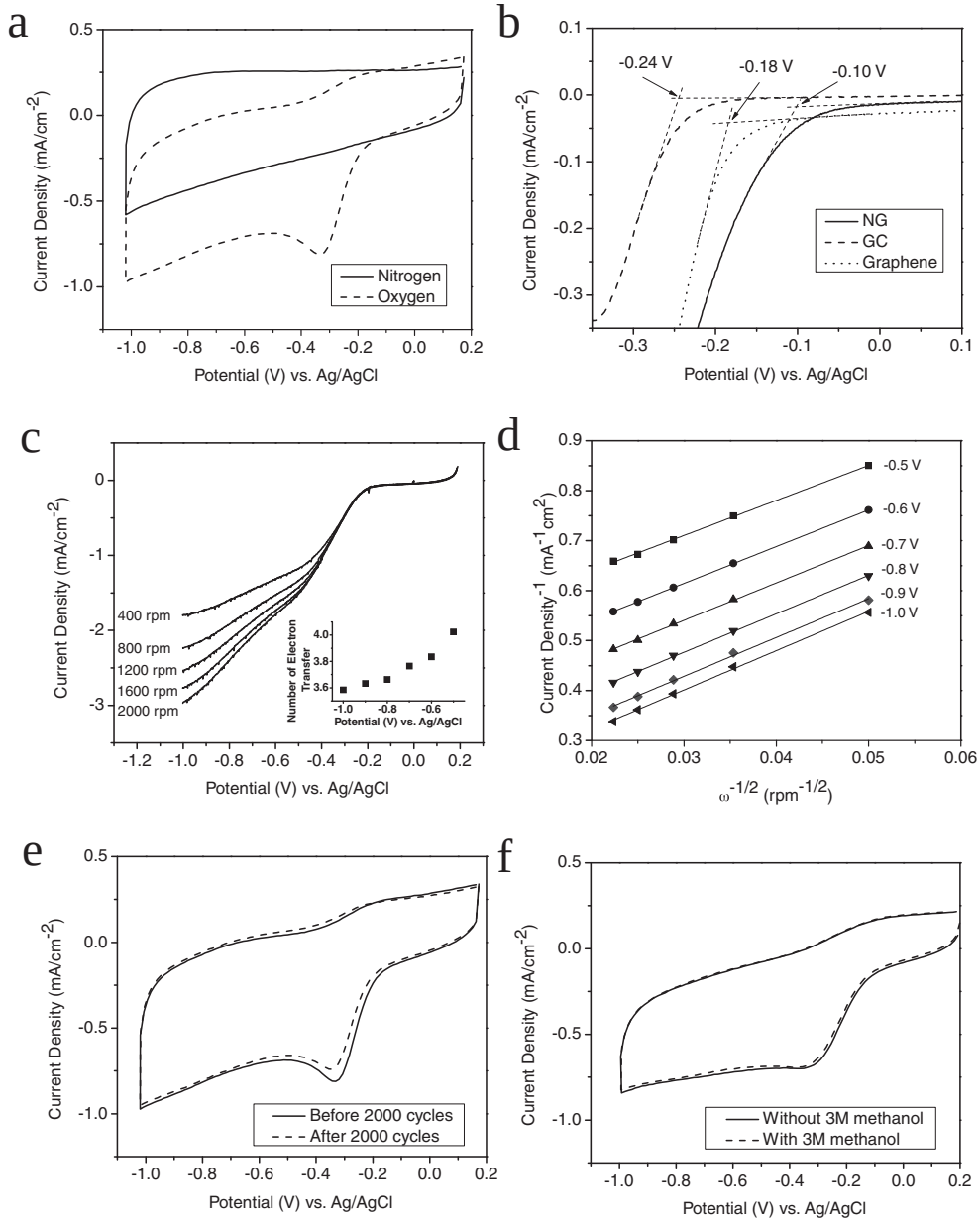

Figure 3. Electrochemical characterizations of NG. a) Cyclic voltammetry (CV) in 0.1 M KOH at a scan rate of 100 mV s^{-1}. b) Linear-scan voltammetry (LSV) of a glassy-carbon (GC) electrode, graphene, NG in 0.1 M oxygen-saturated KOH at scan rates of 10 mV s^{-1}. c) RDE measurements of NG in 0.1 M oxygen-saturated KOH at scan rates of 10 mV s^{-1} (inset: number of electron transfer as a function of potential). d) Koutecky–Levich plots of NG at different electrode potentials. e) CV of NG before and after stability test (2000 cycles in oxygen-saturated 0.1 M KOH at a scan rate of 100 mV s^{-1}). f) CV of NG with and without 3 M methanol (in oxygen-saturated 0.1 M KOH at a a scan rate of 100 mV s^{-1}).

Characterizations: Thermogravimetric analysis (TGA) and DSC were carried out on a simultaneous DSC-TGA analyzer (SDT Q600, TA Instruments Co.). The samples were heated at a rate of 20 °C min^{-1} in nitrogen. SEM (LEO 1530) and TEM (Jeol 100 CX) were used to image the morphology of the NG. FTIR-spectroscopy characterization was performed at ambient temperature using an FTIR spectrometer (Nicolet, Magna IR 560). Raman characterization was carried out using a LabRAM ARAMIS Horiba Jobin Yvon instrument with a 532 nm-wavelength laser. The XPS was carried out using a Thermo K-Alpha XPS instrument. The chemical analysis was performed using a Carlo Erba EA1108 CHN analyzer.

Electrochemical Characterizations: The electrochemical properties of the NG were tested using a three-electrode system. A Pt wire and a Ag/AgCl electrode filled with saturated KCl aqueous solution were used as the counter electrode and reference electrode, respectively. The electrolyte was 0.1 M aqueous KOH solution, which was purged with nitrogen or oxygen for 10 min prior to the electrochemical test. To prepare the NG-loaded working electrode, the NG was dispersed in a mixture of 5 wt% Nafion solution and water (volume ratio = 1:9) by sonication. 1 mg mL^{-1} of the NG dispersion (10.00 μL) was transferred onto a glassy-carbon (GC) electrode (3 mm diameter, 0.07065 cm^2 geometric area) and dried at 80 °C. The NG loading was calculated to be 141 μg cm^{-2}. The control-sample graphene and Pt/C (20 wt.% Pt, Alpha Aesar) on GC were prepared in the same way. The CV and linear-scan-voltammetry (LSV) measurements were performed using a Versastat

2-channel system (Princeton Applied Research). The electrocatalytic activities toward the ORR were also measured using a rotating disk electrode (Pine Instrument, MSR analytical rotator) at a scan rate of 10 mV s^{-1}. The 1 mg mL^{-1} NG dispersion (28 μL) was transferred onto the GC electrode (5 mm diameter, 0.196 cm^2 geometric area) embedded in a polytetrafluoroethylene (PTFE) holder, and dried in air at 80 °C for 1 h. A Pt wire was used as the counter electrode. A 0.1 M KOH solution was prepared as the electrolyte and saturated with oxygen by bubbling with oxygen gas for 30 min before measuring the ORR activities. The potential was controlled using a potentiostat (Solartron, SI 1286).

Supporting Information

Supporting Information is available from the Wiley Online Library or from the author. SEM, XPS of NGs; schematics of the chemical reaction between GO and urea and the structure of NG; discussion on the Raman spectrum of NG; electrochemical characterization of Pt/C.

Acknowledgements

The authors would like to acknowledge financial support from the Natural Science Foundation (NSF, 0800849).

Received: January 14, 2012
Revised: February 29, 2012
Published online: May 11, 2012

[1] K. I. Bolotin, K. J. Sikes, Z. Jiang, M. Klima, G. Fudenberg, J. Hone, P. Kim, H. L. Stormer, *Solid State Commun.* **2008**, *146*, 351.
[2] A. A. Balandin, S. Ghosh, W. Z. Bao, I. Calizo, D. Teweldebrhan, F. Miao, C. N. Lau, *Nano Lett.* **2008**, *8*, 902.
[3] R. R. Nair, P. Blake, A. N. Grigorenko, K. S. Novoselov, T. J. Booth, T. Stauber, N. M. R. Peres, A. K. Geim, *Science* **2008**, *320*, 1308.
[4] K. S. Novoselov, A. K. Geim, S. V. Morozov, D. Jiang, Y. Zhang, S. V. Dubonos, I. V. Grigorieva, A. A. Firsov, *Science* **2004**, *306*, 666.
[5] S. Bae, H. Kim, Y. Lee, X. F. Xu, J. S. Park, Y. Zheng, J. Balakrishnan, T. Lei, H. R. Kim, Y. I. Song, Y. J. Kim, K. S. Kim, B. Ozyilmaz, J. H. Ahn, B. H. Hong, S. Iijima, *Nat. Nanotechnol.* **2010**, *5*, 574.
[6] Z. Y. Lin, Y. Liu, Y. G. Yao, O. Hildreth, Z. Li, K. S. Moon, A. Joshua, C. P. Wong, *J. Phys. Chem. C* **2011**, *115*, 7120.
[7] T. Y. Kim, H. W. Lee, M. Stoller, D. R. Dreyer, C. W. Bielawski, R. S. Ruoff, K. S. Suh, *ACS Nano* **2011**, *5*, 436.
[8] L. T. Qu, Y. Liu, J. B. Baek, L. M. Dai, *ACS Nano* **2010**, *4*, 1321.
[9] D. R. Dreyer, H. P. Jia, C. W. Bielawski, *Angew. Chem. Int. Ed.* **2010**, *49*, 6813.
[10] Y. J. Gao, D. Ma, C. L. Wang, J. Guan, X. H. Bao, *Chem. Commun.* **2011**, 2432.
[11] D. R. Dreyer, H. P. Jia, A. D. Todd, J. X. Geng, C. W. Bielawski, *Org. Biomol. Chem.* **2011**, *9*, 7292.
[12] H. P. Jia, D. R. Dreyer, C. W. Bielawski, *Adv. Synth. Catal.* **2011**, *353*, 528.
[13] H. P. Jia, D. R. Dreyer, C. W. Bielawski, *Tetrahedron* **2011**, *67*, 4431.
[14] D. R. Dreyer, C. W. Bielawski, *Chem. Sci.* **2011**, *2*, 1233.
[15] T. Ikeda, M. Boero, S. F. Huang, K. Terakura, M. Oshima, J. Ozaki, *J. Phys. Chem. C* **2008**, *112*, 14706.
[16] L. P. Zhang, Z. H. Xia, *J. Phys. Chem. C* **2011**, *115*, 11170.
[17] M. Winter, R. J. Brodd, *Chem. Rev.* **2004**, *104*, 4245.
[18] Y. Q. Liu, D. C. Wei, Y. Wang, H. L. Zhang, L. P. Huang, G. Yu, *Nano Lett.* **2009**, *9*, 1752.
[19] L. S. Panchokarla, K. S. Subrahmanyam, S. K. Saha, A. Govindaraj, H. R. Krishnamurthy, U. V. Waghmare, C. N. R. Rao, *Adv. Mater.* **2009**, *21*, 4726.
[20] X. L. Li, H. L. Wang, J. T. Robinson, H. Sanchez, G. Diankov, H. J. Dai, *J. Am. Chem. Soc.* **2009**, *131*, 15939.
[21] D. S. Geng, Y. Chen, Y. G. Chen, Y. L. Li, R. Y. Li, X. L. Sun, S. Y. Ye, S. Knights, *Energy Environ. Sci.* **2011**, *4*, 760.
[22] J. H. Li, Y. Wang, Y. Y. Shao, D. W. Matson, Y. H. Lin, *ACS Nano* **2010**, *4*, 1790.
[23] H. M. Jeong, J. W. Lee, W. H. Shin, Y. J. Choi, H. J. Shin, J. K. Kang, J. W. Choi, *Nano Lett.* **2011**, *11*, 2472.
[24] D. R. Dreyer, R. S. Ruoff, C. W. Bielawski, *Angew. Chem. Int. Ed.* **2010**, *49*, 9336.
[25] A. Gomathi, M. R. Harika, C. N. R. Rao, *Mater. Sci. Eng. A* **2008**, *476*, 29.
[26] A. Gomathi, S. Reshma, C. N. R. Rao, *J. Solid State Chem.* **2009**, *182*, 72.
[27] D. R. Dreyer, S. Park, C. W. Bielawski, R. S. Ruoff, *Chem. Soc. Rev.* **2010**, *39*, 228.
[28] K. N. Kudin, B. Ozbas, H. C. Schniepp, R. K. Prud'homme, I. A. Aksay, R. Car, *Nano Lett.* **2008**, *8*, 36.
[29] D. C. Wei, Y. Q. Liu, Y. Wang, H. L. Zhang, L. P. Huang, G. Yu, *Nano Lett.* **2009**, *9*, 1752.
[30] D. H. Deng, X. L. Pan, L. A. Yu, Y. Cui, Y. P. Jiang, J. Qi, W. X. Li, Q. A. Fu, X. C. Ma, Q. K. Xue, G. Q. Sun, X. H. Bao, *Chem. Mater.* **2011**, *23*, 1188.
[31] S. Stankovich, D. A. Dikin, R. D. Piner, K. A. Kohlhaas, A. Kleinhammes, Y. Jia, Y. Wu, S. T. Nguyen, R. S. Ruoff, *Carbon* **2007**, *45*, 1558.
[32] Z. Lin, Y. Yao, Z. Li, Y. Liu, Z. Li, C. P. Wong, *J. Phys. Chem. C* **2010**, *114*, 14819.
[33] P. A. Schaber, J. Colson, S. Higgins, D. Thielen, B. Anspach, J. Brauer, *Thermochim. Acta* **2004**, *424*, 131.
[34] R. L. Liu, D. Q. Wu, X. L. Feng, K. Mullen, *Angew. Chem. Int. Ed.* **2010**, *49*, 2565.
[35] J. R. Pels, F. Kapteijn, J. A. Moulijn, Q. Zhu, K. M. Thomas, *Carbon* **1995**, *33*, 1641.
[36] M. Seredych, D. Hulicova-Jurcakova, G. Q. Lu, T. J. Bandosz, *Carbon* **2008**, *46*, 1475.
[37] Z. Y. Lin, M. K. Song, Y. Ding, Y. Liu, M. L. Liu, C. P. Wong, *Phys. Chem. Chem. Phys.* **2012**, *14*, 3381.
[38] F. Dong, L. W. Wu, Y. J. Sun, M. Fu, Z. B. Wu, S. C. Lee, *J. Mater. Chem.* **2011**, *21*, 15171.
[39] L. Costa, G. Camino, *J. Therm. Anal.* **1988**, *34*, 423.